

# Primordial black holes and gravitational waves in teleparallel Gravity

K. El Bourakadi<sup>1a</sup>, B. Asfour<sup>2b</sup>, Z. Sakhi<sup>1c</sup>, Z. M. Bennai<sup>1d</sup> and Taoufik Ouali<sup>2e</sup>

<sup>1</sup> Quantum Physics and Magnetism Team, LPMC, Faculty of Science Ben M'sik, Casablanca Hassan II University, Morocco

<sup>2</sup> Laboratory of Physics of Matter and Radiations, Mohammed first University, BP 717, Oujda, Morocco.

Received: date / Revised version: date

**Abstract.** In this paper, we consider the possible effect of the teleparallel gravity on the production of the primordial black holes (PBH) and on the gravitational waves (GWs). We investigate the relationship between the slow roll, the e-folds number and the teleparallel parameters. We show that in the case of the teleparallel parameter  $\delta = 3$ , the e-folds number reaches the values 50 and 60 in consistency with the contour plot of the  $(r, n_s)$  plane obtained by Planck data at  $1\sigma$  and  $2\sigma$  C.L.. Furthermore, we use the fraction of the energy density and the variance of the density perturbations approach to study the abundance of the production PBH. We find that the PBH overproduction can be satisfied for specific values of parameters of the non-adiabatic curvature power spectrum at some narrow parametric resonance. Moreover, to explain the GWs expected by observations, the duration of preheating should be bounded by values less or equal to 2. This bound is in agreement with values of the tensor-to-scalar ratio and the spectral index constrained by Planck data.

**PACS.** PACS-key describing text of that key – PACS-key describing text of that key

## 1 Introduction

General theory of relativity (GR) successfully describes many observational phenomena either at astrophysical [1, 2, 3, 4] and cosmological [5, 6, 7, 8, 9] scales. However, this theory faces many issues such as the standard big bang problems explained in the context of the inflationary paradigm [10, 11]. Indeed, among the most exciting theories that explain the origins of the Universe is the inflation scenario [12, 13, 14]. This paradigm, described through various models, gives a satisfying solution to the standard big bang problems. Accurate measurements of the cosmic microwave background (CMB) and the large-scale structure (LSS) of galaxies provide helpful constraints on this inflationary paradigm [15]. Furthermore, at late-time, General theory of relativity cannot explain the current speed of the expansion of the Universe [16] unless an unknown exotic energy density dubbed Dark energy is introduced. Other observations that form a stumbling block for general relativity may be found in [17, 18, 19]. To overcome these issues, many alternatives to GR have been suggested [20, 21, 22, 23, 24]. An interesting alternatives that has gained more

attention recently are  $f(R)$  gravity [25],  $f(G)$  gravity [26] and  $f(T)$  teleparallel gravity [27, 28, 29, 30]. In this formalism, the geometrical deformation that produces gravitational field is originated by the scalar torsion and not by the scalar curvature. Teleparallel gravity is one of the alternative theories of gravity that gives successful descriptions of the late-time acceleration as well as the inflationary expansion phase [31]. Even though teleparallel gravity reproduces GR in its classical level, many developments of such modified theories has received a lot of attraction [32, 33, 34, 35, 36, 37, 38, 39, 40]. To discriminate among the number of modified theories of gravity, further analysis should be done in order to discard some of those theories which disagree with observations. This alternative theory of GR were considered in many contexts such as in linear perturbations [34, 41], inflation and reheating process [42].

The abundance of primordial black holes (PBH) depends on the primordial power spectrum obtained at the end of inflation and could be considered as a candidate for the formation of dark matter [43, 44, 45, 46, 47]. Indeed, PBH forms due to the amplification in the primordial power spectrum on small scales [48]. Assuming that the Universe has reached the adiabatic limit when it is radiation-dominated, the comoving curvature perturbation is frozen on superhorizon scales. When the scale re-enters the Hubble horizon, some regions may have a large positive curvature which is equivalent to a closed Universe. At this

Send offprint requests to:

<sup>a</sup> k.elbourakadi@yahoo.com

<sup>b</sup> brahim.asfour95@gmail.com

<sup>c</sup> zb.sakhi@gmail.com

<sup>d</sup> mdbennai@yahoo.fr

<sup>e</sup> t.ouali@ump.ac.ma

step the expansion eventually stops and the contraction starts, then the Hubble size region with large positive curvature will collapse to a black hole [48]. Furthermore, it has been argued that after inflation, the inflaton condensate energy density may collapse and forms black holes [49]. After inflation, the Universe enters a reheating era preceded by an era called preheating. In the preheating phase inflaton field began to oscillate and decay into massive bosons due to the parametric resonance. In our model we focus on the preheating period which occurs via a broad parametric resonance. We study the formation of PBH during these period knowing that the scale that exit outside the Hubble radius towards the end of inflation could possibly re-enter the Hubble radius after reheating during the radiation dominated era. However, amplified fluctuations during preheating lead to PBH formation on the slightly shorter scales which re-enter the Hubble radius during preheating [50]. Moreover, these amplifications during the preheating process can lead to the amplification of sufficiently large curvature perturbations and lead to the overproduction of primordial black holes [50]. The imprints that PBH may leave in observations provide an important background to some astrophysical issues. Indeed, these signatures may interpret the non linear seeds of the large scale structure and the PBH evaporation could explain the point-like gamma-ray sources [51,52].

On the other hand, gravitational waves, which is theoretically predicted by general relativity, is originated from astronomical objects or by the dynamical expansion of the early Universe. While merging black hole or colliding neutron stars may describe the first generation, the so called primordial GWs are generated in the early Universe. In this paper, we consider the second generation of GWs which is generated during the inflationary era by means of the enhancing of the primordial curvature perturbations. However, a significant production of GWs is sourced in the preheating era characterized by the parametric resonance [54,55]. These GWs leave an indirect imprint in the cosmic microwave background temperature anisotropies, specially in the measurement of its polarization [53]. At the end of inflation, inhomogeneities of the time-dependent field act as a gravitational source and the spectrum of GWs can be linked directly to the duration of preheating. Inflationary scenario predicts such GWs and their detection, whether directly or indirectly, can provide us a unique opportunity to test theories of inflation [56]. The amplitude of the GWs spectrum, which is generated during preheating, is independent of the energy scale of inflation characterizing the present peak frequency of the GWs spectrum [57,58].

Motivated by the increasing interest in teleparallel gravity, we study the production of the primordial black hole, the constraints of the amplitude of the scalar primordial on the parameters of the model. The gravitational waves are also considered in this context. To this aim, we introduce the inflationary paradigm and relate its parameters to the subsequent era namely the preheating and the re-

heating phases.

The paper is organized as follows: In Sec. 2, we setup the basic concept of teleparallel gravity and introduce some fundamental parameters of the inflationary scenario. In Sec. 3, we constrain the e-fold parameter of the preheating era to those of inflationary paradigm. In Sec. 4, we derive the reheating phase in terms of the e-folds number  $N_{re}$ , we briefly discuss the perturbative process of reheating and highlight the correlation of  $f(T)$  model parameters and the reheating duration. In Sec. 5, we introduce the primordial black holes and their production by means of model parameters. In Sec. 6, we study the production of the gravitational waves and their constraints from observations. Sec. 7 is dedicated to conclusions.

## 2 Teleparallel gravity and inflationary parameters

As an alternative formulation of gravity, teleparallel gravity is a theory formulated in terms of torsion with no curvature term [59]. The fundamental orthonormal field which maps space-time coordinates  $x^\mu$  to the coordinates  $x^a$  on the tangent-space is the tetrad  $e^a{}_\mu$ . In terms of the tetrad, the space-time metric can be expressed as follows [60]

$$g_{\mu\nu} = \eta_{ab} e^a{}_\mu e^b{}_\nu,$$

where  $\eta_{ab}$  is the Minkowski metric. The tetrad obeys normalization conditions  $e^a{}_\mu e_b{}^\mu = \delta_b^a$  and  $e^a{}_\mu e_a{}^\nu = \delta_\mu^\nu$ . The Latin and Greek indices stand for tangent space and space-time coordinates, respectively. Modified gravity can also be constructed by a given action based on teleparallel gravity. We construct the modified teleparallel gravity by an action depending on the torsion scalar  $T$ , minimally coupled to a barotropic fluid described by the scalar field,  $\phi$ , and the radiation's Lagrangian density,  $\mathcal{L}_r$ . The action under consideration is then given by [61]

$$S = \int d^4x \sqrt{-g} \left[ \frac{M_p^2}{2} f(T) + \frac{1}{2} \partial_\mu \phi \partial^\mu \phi - V(\phi) + \mathcal{L}_r \right], \quad (1)$$

where  $g$  is the determinant of the metric. The torsion scalar  $T$  is constructed by a contraction of the torsion tensor

$$T = \frac{1}{4} T_{\rho\mu\nu} T^{\rho\mu\nu} + \frac{1}{2} T^{\nu\mu\rho} T_{\rho\mu\nu} - T_{\rho\mu}{}^\rho T^{\nu\mu}{}_\nu \quad (2)$$

with the torsion tensor given by

$$T_{\mu\nu}^\gamma = \Gamma_{\mu\nu}^\gamma - \Gamma_{\nu\mu}^\gamma = e_a{}^\gamma (\partial_\mu e^a{}_\nu - \partial_\nu e^a{}_\mu). \quad (3)$$

In the context of the flat Friedmann-Lemaître-Robertson-Walker (FLRW) metric

$$ds^2 = -dt^2 + a^2(t) (dr^2 + r^2(d\theta^2 + \sin^2\theta d\phi^2)), \quad (4)$$

the tetrad field of a FLRW Universe is given by

$$e^a{}_\mu = \text{diag}(1, a(t), a(t), a(t)), \quad (5)$$

and the modified Friedman equations in teleparallel gravity are

$$H^2 = \frac{1}{3M_p^2} (\rho_\phi + \rho_r + \rho_T), \quad (6)$$

$$\dot{H} = -\frac{1}{2M_p^2} (\rho_\phi + \rho_r + \rho_T + P_\phi + P_r + P_T), \quad (7)$$

where  $H$  and  $\dot{H}$  are the Hubble parameter and its differentiation with respect to the cosmic time  $t$ . The energy density of the scalar field and its pressure are given by  $\rho_\phi = \dot{\phi}^2/2 + V(\phi)$  and  $P_\phi = \dot{\phi}^2/2 - V(\phi)$ , respectively.  $\rho_r$  and  $P_r$  are the energy density and the pressure of radiation. In the FLRW, the torsion scalar is related to the Hubble parameter as  $T = -6H^2$ , the energy density  $\rho_T$  and the pressure  $P_T$  are written as [61]

$$\rho_T = \frac{M_p^2}{2} (2T f_{,T} - f - T), \quad (8)$$

$$P_T = -\frac{M_p^2}{2} (-8\dot{H}T f_{,TT} + (2T - 4\dot{H}) f_{,T} - f + 4\dot{H} - T), \quad (9)$$

where

$$f_{,T} = \frac{\partial f(T)}{\partial T} \quad \text{and} \quad f_{,TT}(T) = \frac{\partial^2 f}{\partial T^2}. \quad (10)$$

In order to analyze preheating parameters, we introduce the model used in [42] to derive the inflationary parameters that are directly linked to inflation parameters. Usually preheating is characterized by the production of  $\chi$ -particles through the parametric resonance which could be either narrow or broad resonance depending on a specific condition on the parameters of the well-known Mathieu equation that describe  $\chi$ -field evolution. To illustrate our purpose, we consider a power-law modified teleparallel [62]

$$f(T) = CT^{1+\delta}, \quad (11)$$

where  $\delta$  is a positive integer and  $C = 1/M^{2\delta}$  with  $M = 10^{-4}M_p$  is a mass dimension constant. For later uses, we give the background and the perturbative parameters in the slow-roll approximation. The first and the second slow-roll parameters, defined as  $\epsilon_1 = -\dot{H}/H^2$  and  $\epsilon_2 = \dot{\epsilon}_1/H\epsilon_1$ , are given by [62]

$$\epsilon_1 = -\frac{(-M_p^2 C (\delta + \frac{1}{2}))^{(\frac{1}{1+\delta})}}{(1+\delta)} \frac{V'(\phi)^2}{V(\phi)^{\frac{\delta+2}{\delta+1}}}, \quad (12)$$

$$\epsilon_2 = 2\epsilon_1 \left( (2+\delta) - 2(1+\delta) \left( \frac{V''(\phi)V(\phi)}{V'(\phi)^2} \right) \right). \quad (13)$$

The e-folds number of inflation considered from the time of the horizon crossing to the inflation's end, labeled by the index "k" and "end" respectively, is written as

$$N_I \simeq -\int_{\phi_k}^{\phi_{end}} \frac{3H^2}{V'(\phi)} d\phi = \frac{2^{-\frac{\delta}{1+\delta}}}{(M_p^2(-1)^\delta C(1+2\delta))^{\frac{1}{1+\delta}}} \int_{\phi_{end}}^{\phi_k} \frac{V(\phi)^{\frac{1}{1+\delta}}}{V'(\phi)} d\phi. \quad (14)$$

The spectral index and the power spectrum are given by [62]

$$n_s - 1 \simeq -2\epsilon_1 - \epsilon_2, \quad (15)$$

$$\mathcal{P}_s \simeq \left( \frac{H_k^2}{8\pi^2 M_p^2 c_s^3 \epsilon_1} \right)_{c_s k = aH}, \quad (16)$$

where  $c_s$  denotes the sound speed and the power spectrum is evaluated at the horizon crossing i.e. at  $c_s k = aH$ . The sound speed for our suggested model is

$$c_s^2 = \frac{f_{,T}}{f_{,T} + 12H^2 f_{,TT}} = \frac{1}{1+2\delta}. \quad (17)$$

The relation between inflationary parameters and cosmological perturbations provides a useful way to constrain preheating parameters for a chosen model of inflation. For the case of chaotic potential  $V = m^2 \phi^2/2$  which is recently argued that is the simplest and perhaps the most elegant model [63], the solution to the well known Klein Gordon equation corresponding to the inflaton field is given by  $\phi = \Phi \cdot \sin mt$  with  $m$  is the inflaton mass and  $\Phi$  is the initial amplitude of the  $\phi$ -field oscillations. The spectral index for the chaotic potential is given by  $n_s - 1 \simeq -4\epsilon_1$  since  $\epsilon_2 = 2\epsilon_1$ . Next, we compute preheating parameters, in particular, the inflationary e-folds  $N_I$ , the Hubble parameter during inflation  $H_k$  and the potential at the end of inflation  $V_e$ . The e-folds number during inflation can be calculated as

$$N_I = 4 \cdot \frac{(-1)^{\frac{2}{1+\delta}}}{(1-n_s)(\delta-1)}. \quad (18)$$

In order to calculate the Hubble parameter  $H$ , one needs to compute the power spectrum given by [42]

$$\mathcal{P}_s \simeq \left( -\frac{(-M_p^2 C (\frac{1}{2} + \delta))^{\frac{2\delta}{1+\delta}} (1+\delta) M_p^2 V(\phi)^{\frac{3-\delta}{1+\delta}}}{12\pi^2 C^2 M_p^6 \sqrt{1+2\delta} \alpha^2 V'(\phi)^2} \right)_{c_s k = aH}, \quad (19)$$

which in the case of chaotic inflation writes

$$\mathcal{P}_s \simeq -\frac{8}{3} \frac{m^2}{\pi^2 C^2 M_p^6 \sqrt{1+2\delta}} \frac{(-M_p^2 C (\frac{1}{2} + \delta))^2}{(1+\delta)(1-n_s)^2}, \quad (20)$$

knowing that  $\epsilon_1 = (1-n_s)/4$ , Eq. (16) can be rewritten as

$$H_k^2 \simeq 2\pi^2 M_p^2 c_s^3 \mathcal{P}_s (1-n_s). \quad (21)$$

Inflation ends when the slow-roll parameter  $|\epsilon_1(\phi_{end})| \approx 1$  and the value of the field at the end of inflation writes

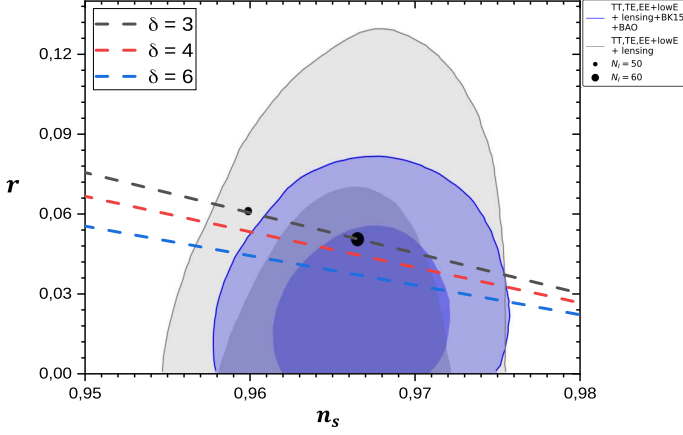


Fig. 1:  $r$  as a function of  $n_s$  for a chaotic potential in modified teleparallel gravity. Inner and outer shaded regions are  $1\sigma$  and  $2\sigma$  constraints in combination with CMB lensing reconstruction and BAO from Planck data, respectively. We choose three different values of  $\delta$ , the black line for  $\delta = 3$ , the red line represents  $\delta = 4$  and the blue line for  $\delta = 6$ . The dots correspond to 50 and 60 inflationary e-folds for the case of  $\delta = 3$ , respectively.

$$\phi_{end}^2 = 2^{\delta+2} \left( \frac{1}{1+\delta} \right)^{1+\delta} \left( M_p^2 C m^{2\delta} \left( \frac{1}{2} + \delta \right) \right). \quad (22)$$

An essential inflationary parameter is the tensor-to-scalar ratio which is given, in teleparallel gravity, by [62]

$$r = 16c_s^3 \epsilon_1. \quad (23)$$

The observable quantities  $r$  and  $n_s$  can also be obtained in terms of  $N_I$  as

$$r = \frac{16}{N_I (\delta - 1) \sqrt{1 + 2\delta}}, \quad n_s - 1 = -\frac{4}{N_I (\delta - 1)}. \quad (24)$$

Considering the chaotic potential in our chosen teleparallel gravity, Fig. (1) shows that the tensor-to-scalar ratio,  $r$ , is a decreasing function with respect to the spectral index,  $n_s$ . The results show a good consistency for a specific range of model parameters with the latest observations from Planck data. Moreover, in the case of  $\delta = 3$ , the choice of 50 and 60 inflationary e-folds produces consistent observational parameters with recent results. Finally, since  $N_I$ ,  $H$ , and  $V_e$  are expressed as functions only of  $\delta$  and  $n_s$ , one may extend the investigation to the preheating parameter  $N_{pre}$  and to the so-called non-adiabatic curvature  $\zeta_{nad}$  that arises from  $\chi$  field perturbation. The next section will be devoted to this task.

### 3 Constraints on preheating parameters

In order to describe preheating through the parametric resonance, one would introduce a preheating field  $\chi$ . During preheating the potential gets an additional term [64]

$$V(\phi, \chi) = m^2 \phi^2 / 2 + g^2 \phi^2 \chi^2 \quad (25)$$

with  $g$  is the coupling of the inflaton to the  $\chi$  field. After inflation, amplified quantum fluctuations in  $\chi$  field obey the wave equation [66]

$$\delta \ddot{\chi} + 3H \delta \dot{\chi} + \left( \frac{k^2}{a^2} + g^2 \phi^2 \right) \delta \chi = 0, \quad (26)$$

where  $k$  is the comoving wavenumber and  $a$  is the scale factor. The  $\chi$  field with the effective mass results in an efficient preheating with large amplitude oscillations when  $q \equiv g^2 \Phi^2 / 4m^2 \gg 1$ . The growth of the  $\chi$  field fluctuations during preheating gives rise to the non-adiabatic curvature perturbation  $\zeta_{nad}$ . Since the inflaton decay can violate the adiabatic condition during preheating, pressure perturbations can be split into adiabatic and non-adiabatic parts and the evolution of  $\zeta$  arises from the non-adiabatic part of pressure perturbations. Moreover, the non-adiabatic perturbations can cause a change in  $\zeta$  on arbitrarily large scales when non-adiabatic pressure perturbations are non-negligible. In fact, variations of  $\zeta$  during preheating could be driven by the non-adiabatic part of the  $\chi$  field perturbation. The power spectrum resulting from this amplification is given by [66, 64]

$$\mathcal{P}_{\zeta_{nad}} \simeq \frac{29/23}{\pi^5 \mu^2} \left( \frac{\Phi}{M_P} \right)^2 \left( \frac{H_{end}}{m} \right)^4 \frac{g^4}{q^{1/4}} \left( \frac{k}{k_{end}} \right)^3 I(\kappa, m\Delta t), \quad (27)$$

where, by defining  $\kappa^2 \equiv \frac{1}{18\sqrt{q}} \left( \frac{k}{k_{end}} \right)$ ,

$$I(\kappa, m\Delta t) \equiv \frac{3}{2} \int_0^{\kappa_{cut}} d\kappa' \int_0^\pi d\theta e^{2(\mu_{\kappa'} + \mu_{\kappa - \kappa'}) m\Delta t} \kappa'^2 \sin(\theta), \quad (28)$$

here  $\theta$  is the angle between  $\kappa'$  and  $\kappa$ ,  $\kappa_{cut}$  is an ultraviolet cut-off. The comoving wavenumber at the Hubble radius exit and at the end of inflation are denoted by  $k$  and  $k_{end}$ , respectively. The term  $m\Delta t$  is an alternative way to estimate how long the process of preheating will proceed and  $\mu = (\ln 3)/2\pi$  for  $q \gg 1$ . At the end of inflation when  $m\Delta t = 0$ , the integral appeared in the power spectrum  $\mathcal{P}_{\zeta_{nad}}$  is estimated to  $I(\kappa, 0) = \kappa_{cut}^3 \sim 1$  [64].

From Eq.(27),  $H_{end}$  is determined through the modified Friedmann equation due to the teleparallel gravity under consideration and is given by [42]

$$H_{end}^2 = \frac{2^{-\frac{\delta}{\delta+1}}}{3} \left( \frac{V_e}{3(-1)^\delta M_p^2 C (1+2\delta)} \right)^{\frac{1}{1+\delta}}. \quad (29)$$

The amplitude of non-adiabatic curvature perturbations  $\mathcal{P}_{\zeta_{nad}}$  is displayed as a function of  $k/k_{end}$  in Fig. (2), for  $\delta = 3, 4, 6$ ,  $m\Delta t = 0$  and  $I(\kappa, 0) = 1$ . One

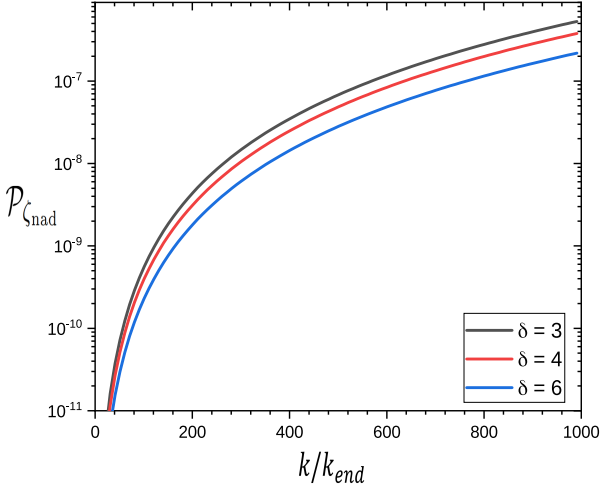


Fig. 2: The non-adiabatic curvature perturbation  $\mathcal{P}_{\zeta_{nad}}$  is presented for different  $\delta$  values,  $\delta = 3, 4$  and  $6$ . The other parameters are given as :  $\Phi \simeq M_p/\sqrt{12\pi}$ ,  $g = 10^{-3}$ ,  $m = 10^{-6}M_p$ ,  $q = 6600$ .

can check that when  $k/k_{end} \rightarrow 0$ , the power spectrum is in the order of  $\sim 10^{-11}$ . On the other hand, when the ratio  $k/k_{end}$  increases the power spectrum increases towards values higher than  $\sim 10^{-7}$ . Since  $\mathcal{P}_{\zeta_{nad}} \propto k^3$ , when  $k \sim k_{end}$  and  $m\Delta t \neq 0$  the change in  $\zeta$  is weakly affected for the large scale structure to be formed due to the preheating. In fact, small scale fluctuations may become large enough for PBH to be overproduced [66]. We will discuss this in more detail in the next section. Furthermore, extracting informations about preheating requires considering the phase between the scale at the horizon crossing during inflation to the present time, which can be derived in terms of inflationary parameters as [67, 73]

$$N_{pre} = \left[ 61.6 - \frac{1}{4} \ln \left( \frac{V_e}{\gamma H^4} \right) - N_I \right] - \frac{1-3\omega}{4} N_{re}, \quad (30)$$

where the parameter  $\gamma$  is assumed to relate the energy density at the end of inflation,  $\rho_e$ , to the preheating energy density,  $\rho_{pre}$ . The reheating duration  $N_{re}$  can be obtained from reheating energy density  $\rho_{re} = (\rho_e/\gamma) e^{-3(1+\omega)N_{re}}$  [67], with  $\rho_{re} = (\pi^2/30) g_* T_{re}^4$  and  $g_*$  denotes the number of relativistic degrees of freedom at the end of reheating [67]

$$N_{re} = \frac{1}{3(1+\omega)} \ln \left( \frac{3^2 \cdot 5 V_e}{\gamma \pi^2 g_* T_{re}^4} \right). \quad (31)$$

We provide a numerical evaluation of the duration of preheating for the case of chaotic potential in the modified teleparallel inflation as shown in Fig. (3). We choose the EoS parameter to be  $\omega \simeq 1/4$  following the assumption that during preheating the EoS gets closer to  $1/3$  [67],

we take also a fixed value of  $\delta = 3$  following constraints on the inflationary e-folds found in the previous section. We observe that the preheating duration is weakly sensitive to the reheating temperature and is weakly shifted to the right for higher values of the parameter  $\gamma$ . From Eq. (30), lower values of reheating temperature allow a minimum value of the preheating duration. In this direction, we choose two cases of the final reheating temperature, the first one in order of  $\sim 10^{12} GeV$  and the second one in order of the electroweak scale  $\sim 100 GeV$ . Both cases in the figure (3) show a good consistency with recent observation results since all lines fall toward the central value of the observational bound [15]. We notice that from Eq. (31) the maximum reheating temperature is bounded as  $T_{re} \sim [10^{12} - 10^{13}]$  where reheating is defined to be instantaneous. However, we consider a lower case where the reheating occurs at the electroweak scale to test the thermalization temperature effects on the reheating duration. In this model, preheating could appear either instantaneously or reach  $N_{pre} \sim 10$  to  $14$  e-folds depending on the choice of  $T_{re}$  and  $\gamma$  parameter. On the other hand, in our setup, preheating scenario is very sensitive to the  $\delta$  parameter of the chosen teleparallel model  $f(T)$ . In fact, the main reason behind the choice of  $\delta = 3$  is the inflationary e-folds number  $N_I$  that will take higher values when  $\delta > 3$  which is inconsistent with Planck observation as shown in Fig. (1). Hence, higher values of  $N_I$  affects the preheating duration (see: Eq. (30)) and makes the curves fall away from the central bound on  $n_s$ .

## 4 Reheating in modified teleparallel gravity

During preheating, the oscillating inflaton field decays into massive bosons  $\chi$ . However, it is preferred that there will be no explosive creation of fermions taking into consideration the Pauli exclusion principle [68]. The explosive particles production during this step is due to the parametric resonance when the amplitude of the inflaton field and the coupling constants became large. From the measurements of CMB anisotropies we know that the Universe reheated by reaching a thermal equilibrium in the beginning of the big-bang nucleosynthesis (BBN) with a temperature satisfying  $T_{re} > T_{BBN}$  [69], this reheating phase occurred from the end of preheating at  $a = a_{pre}$  and ended at  $a = a_{re}$ . Usually reheating is discussed through perturbative approach [70, 71] which describe the inflaton decay into relativistic bosonic and fermionic particles. This decay is explained by inserting the friction term  $\Gamma \dot{\phi}^2$  into the inflaton equation of motion, where  $\Gamma$  is the decay rate [72].

During inflation, the scalar field decreases very slowly, and then after the slow roll, a rapid oscillation starts at reheating phase, which generates relativistic particles. The produced relativistic particles become dominant and compose a state of thermal equilibrium fluid. During this rapid oscillation until the radiation dominance, we can quantify the reheating phase by the duration  $N_{re}$  which takes into consideration the parameters of our chosen modified

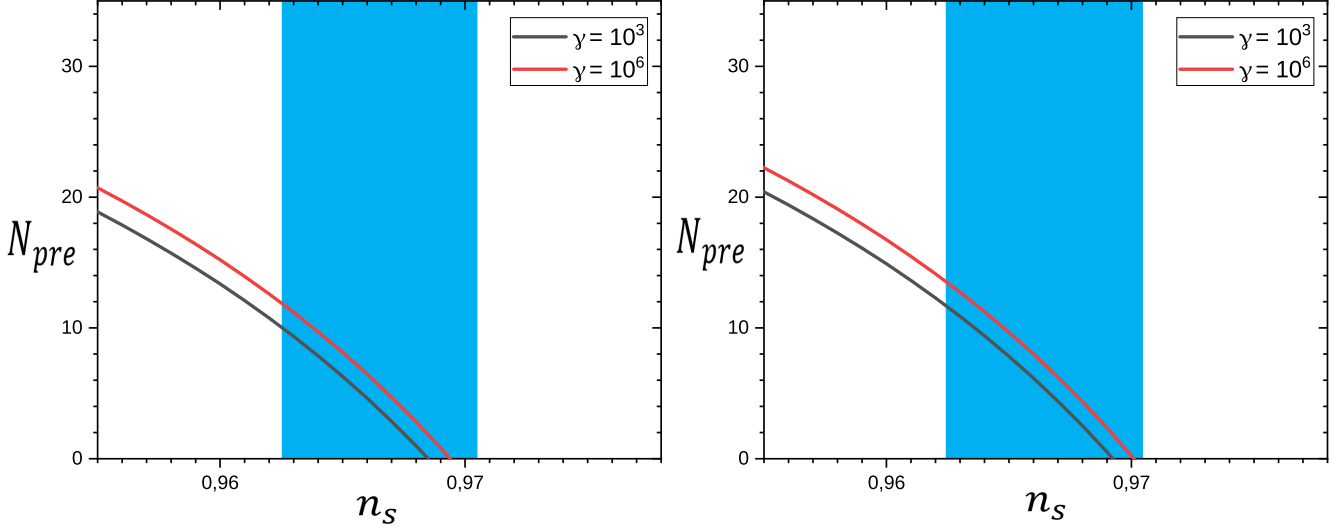


Fig. 3: The preheating  $N_{pre}$  as functions of  $n_s$  for chaotic inflation. We choose  $\gamma$  to be  $\gamma = 10^3$  and  $\gamma = 10^6$ . The blue region represents Planck's bound on  $n_s$ . In the left panel, we considered the temperature  $T_{re} = 10^{12} \text{ GeV}$ , while in the right one, we choose a minimal reheating temperature  $T_{re} = 100 \text{ GeV}$ .

teleparallel model of gravity. Knowing that energy densities at the end of preheating and reheating respectively are given by  $\rho_{re} \propto a_{re}^{-3(1+\omega)}$  and  $\rho_{pre} = \rho_{end}/\gamma = a_{pre}^{-3(1+\omega)}$  [67]. The decay rate is given in terms of the reheating temperature  $T_{re}$  and the number of relativistic degrees of freedom  $g_*$  by [69]

$$\Gamma^2 \simeq \frac{\pi^2}{10M_p^2} g_* T_{re}^4. \quad (32)$$

Hence, the duration of reheating is derived as

$$\begin{aligned} N_{re} &= \ln \left( \frac{a_{re}}{a_{pre}} \right) \\ &= \frac{-1}{3(1+\omega)} \ln \left( \frac{\frac{2}{3}\gamma\Gamma^2}{2^{\delta+2} \left( \frac{1}{1+\delta} \right)^{1+\delta} M_p^2 C m^{2+2\delta} \left( \frac{1}{2} + \delta \right)} \right). \end{aligned} \quad (33)$$

This analysis about reheating is based on the original studies of perturbative reheating after inflation where the ultra-relativistic particles are gradually produced until the radiation era begins to dominate. Our reheating duration result is compatible with the existence of a primary preheating phase that is studied by non-perturbative methods. Here we suppose that at this step the EoS is still moving towards  $\omega = 1/3$  where the radiation era takes place.

## 5 Primordial black hole production

Preheating is the period of the broad parametric resonance which occurs at the end of inflation and before reheating. In addition, preheating is characterized by amplified  $\chi$  field fluctuations that are responsible for a non-adiabatic curvature perturbation  $\zeta_{nad}$ . The formation of PBH in the early Universe is usually due to a collapse of large density perturbations [74]. Some observational constraints on PBH abundance have been considered in [75, 76] and were estimated to be less than  $10^{-20}$  of the total energy density of the Universe. An important condition that must be satisfied is that the density contrast must exceed the critical value  $\delta_c = 0.414$  [77] in order for PBH to be formed during the radiation domination era when fluctuations enter the horizon. PBH production is estimated by means of the fraction of the energy density which in turns is related to the variance of the density perturbation. To this aim, we use the power spectrum and a window function  $W(kR)$  [48], to define the variance  $\sigma(k)$

$$\sigma^2(k) = \frac{16}{81} \int_0^\infty \left( \frac{\tilde{k}}{k} \right)^4 \mathcal{P}_{\zeta_{nad}}(\tilde{k}) W^2(\tilde{k}R) \frac{d\tilde{k}}{\tilde{k}}, \quad (34)$$

where the comoving horizon length  $R = 1/k$  is the scale at which the variance is assumed to be coarse-grained. The

window function has a Gaussian form given by

$$W(\tilde{k}R) = \exp\left(-\frac{\tilde{k}^2 R^2}{2}\right). \quad (35)$$

The final form of the variance of the density perturbations is obtained as [50]

$$\sigma^2(k) \approx 10\sqrt{2\pi} \frac{2^{9/2} 3}{\pi^5 \mu^2} \left(\frac{\Phi}{M_p}\right)^2 \left(\frac{H_{end}}{m}\right)^4 g^4 q^{1/2} \left(\frac{k}{k_{end}}\right)^3 I(\kappa, m\Delta t). \quad (36)$$

Evaluating Eq. (36), we plot the mass variance  $\sigma(k)$  at the horizon crossing in Fig. (4) as a function of the wavenumber ratio  $k/k_{end}$  for several values of  $\delta$ . According to [66] at later times of preheating, the integral appearing in Eq. (28) is calculated as

$$I(\kappa, m\Delta t) = 0.86(m\Delta t)^{-3/2} e^{4\mu m\Delta t}. \quad (37)$$

We find that for  $k/k_{end} \leq 10^{-1}$  and  $m\Delta t = 25$ , the variance does not exceed the threshold value with  $\sigma_{thresh} = 0.08$  [64,65] at which the overproduction of PBH occurs. However, for the case  $m\Delta t = 50$  and  $k/k_{end} \leq 10^{-1}$ , the overproduction of PBH take place for  $\delta = 3, 4$  as  $\sigma \geq \sigma_{thresh}$ .

Assuming that primordial curvature perturbations follows Gaussian distributions lead to estimating the abundance of PBH [48]. The fraction of the energy density that collapses into PBH is estimated as [74]

$$\beta(k) = \frac{1}{2} \text{Erfc}\left(\frac{\delta_c}{\sqrt{2}\sigma(k)}\right). \quad (38)$$

The complementary error function can be approximated so that the energy density fraction can be rewritten as [78, 77]

$$\beta(k) \simeq \sqrt{\frac{1}{2\pi}} \frac{\sigma}{\delta_c} \exp\left(-\left(\frac{\delta_c}{\sqrt{2}\sigma(k)}\right)^2\right). \quad (39)$$

One important question is whether PBH are large enough to explain the LIGO-Virgo events. For this reason, the fraction of the energy density can give an alternative explanation to study PBH collapses in the early Universe. Fig. (5) shows the fraction of the total energy density for spherically symmetric regions collapsing into PBH as a function of the dimensionless wavenumber  $k/k_{end}$ . The results show that the curves converge toward  $10^{-1}$  for  $m\Delta t = 50$  where the overproduction of PBH is less probable. However, for an overproduction regime where  $m\Delta t = 65$ , PBH production is satisfied for  $\delta = 3, 4$  and 6 when  $k/k_{end} \geq 0.015$ .

## 6 Gravitational Waves production

In this section we discuss Gravitational Waves production in  $f(T)$  gravity. The intense production of matter fields after inflation can promote substantial metric changes. However, instead of the symmetric metric field, we only focus

on the tetrad field and the generation of GWs during preheating. Since gravitational waves are detected through line element change we no longer consider 10 components of the metric tensor, instead, the 16 components of the tetrads must be taken into consideration and the tetrad  $e_\mu^a$  will have an additional tangent space-time indices [79, 80]. The metric satisfies the condition

$$g_{\mu\nu} = \eta_{ab} e_\mu^a e_\nu^b = \eta_{ab} \bar{e}_\mu^a \bar{e}_\nu^b, \quad (40)$$

and the tetrad can be decomposed as

$$e_\mu^a = \bar{e}_\mu^a + \chi_\mu^a, \quad (41)$$

where  $\bar{e}_\mu^a$  represents the part corresponding to metric components, and  $\chi_\mu^a$  illustrates the degrees of freedom obtained from the local Lorentz transformation. Focussing only on the  $\bar{e}_\mu^a$  part, which can be perturbed around the flat FLRW background that gives rise to metric perturbations. We can obtain the perturbed torsion tensor from these calculations that lead to perturbations in the field equations from which the equation of motion for the GWs writes [81]

$$\ddot{h}_{ij} + \left(3H + \frac{\dot{f}_{,T}}{f,T}\right) \dot{h}_{ij} - \frac{\nabla^2}{a^2} h_{ij} = 0 \quad (42)$$

The energy density carried by GWs and sourced by the inhomogeneous decay of the symmetry breaking field is given by [82]

$$\rho_{GW} = \frac{M_p^2}{4} \langle \dot{h}_{ij}(t, x) \dot{h}_{ij}(t, x) \rangle \quad (43)$$

the abundance of gravity waves energy density today is presented by the energy spectrum given as [82]

$$h^2 \Omega_{GW,0}(f) = \frac{h^2}{\rho_{c,0}} \frac{d\rho_{GW,0}}{d \ln f}, \quad (44)$$

where  $h$  is the present dimensionless Hubble constant,  $f$  is the frequency and  $\rho_{c,0} = 3H_0^2/(8\pi G)$  is the current critical energy density. Considering the scale factor at the present time,  $a_0$ , and at the time when GWs production stops,  $a_{end}$ , the GWs spectrum can be converted into the actual physical quantities in order to correlate the density spectrum with current observations [82]

$$\frac{a_{end}}{a_0} = \frac{a_{end}}{a_{pre}} \left(\frac{a_{pre}}{a_{re}}\right)^{1-\frac{3}{4}(1+\omega)} \left(\frac{g_*}{g_0}\right)^{-\frac{1}{12}} \left(\frac{\rho_{r,0}}{\rho_*}\right)^{\frac{1}{4}}, \quad (45)$$

here we consider that at the end of preheating "pre" GWs production stops. "0" and "re" indicate the present time

and the time when reheating is finished, respectively.  $\rho_*$  and  $\rho_{r,0}$  are the total energy density of the scalar field and the current radiation energy density, respectively. The present GWs spectra can finally be given in the form [67]

$$\Omega_{GW,0} h^2 = e^{-4N_{pre}} \left(\frac{g_*}{g_0}\right)^{-\frac{1}{3}} \Omega_{r,0} h^2 \Omega_{GW}(f), \quad (46)$$



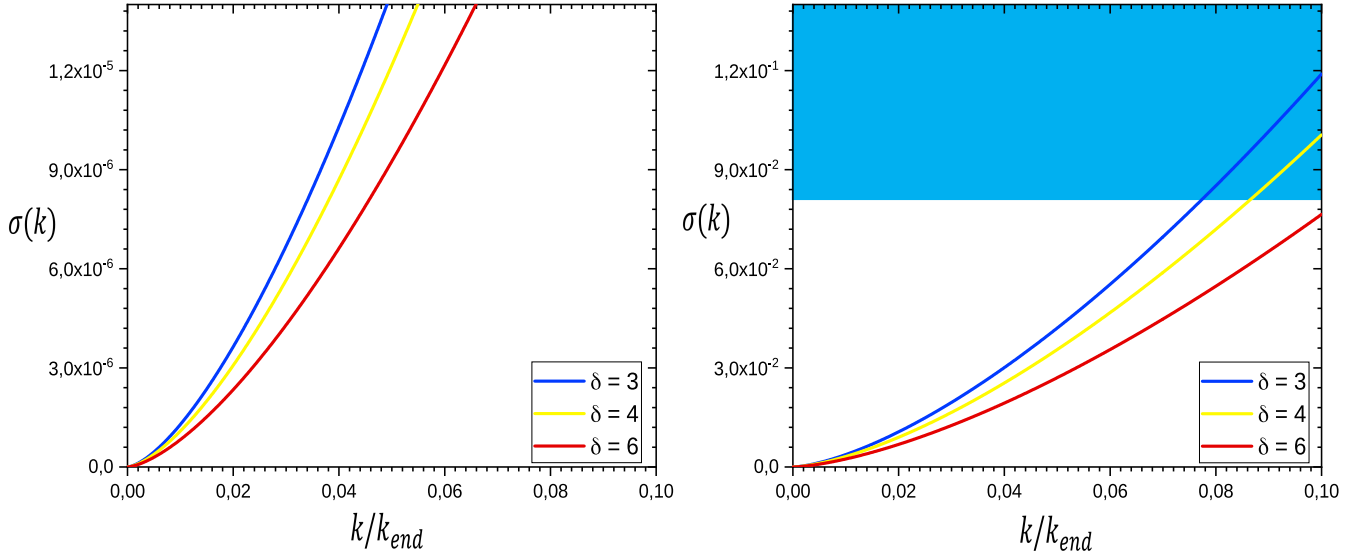


Fig. 4: The mass variance  $\sigma(k)$  as a function of dimensionless wavenumber  $k/k_{end}$ , for  $\delta = 3$  (blue-line),  $\delta = 4$  (yellow-line),  $\delta = 6$  (red-line),  $\Phi \simeq M_p/\sqrt{12\pi}$ ,  $g = 10^{-3}$ ,  $m = 10^{-6}M_p$  and  $q = 6600$ . The blue region shows the threshold  $\sigma_{thresh} = 0.08$  at which PBH are overproduced. The left panel presents the case of  $m\Delta t = 25$ , while in the right panel  $m\Delta t = 50$ .

Eq. (46) is obtained by considering that during preheating the equation of state jumps from  $\omega = 0$  to an intermediate value close to  $\omega = 1/3$ . Furthermore,  $\omega$  will reach  $1/3$  just after preheating [83] which leads to  $(a_{pre}/a_{re})^{1-1/4(1+\omega)} = 1$ . The current density fraction of radiation  $\Omega_{r,0} = \rho_{r,0}/\rho_{c,0}$  is given by  $\Omega_{r,0} \simeq 9.1 \times 10^{-5}$ .  $\Omega_{GW,0}h^2 \propto 1/a_0^4 g_*$  and  $g_0$  satisfies  $g_*/g_0 \simeq 106.75/3.36 \simeq 31$ . The recent analysis of 12.5-year of PTA published by the NANOGrav collaboration shows a stochastic GWs behaviour. this analysis suggests a power-law type of the strain of the GWs [84, 85, 86, 87]

$$\Omega_{GW}(f) = \frac{2\pi^2 f_{yr}^2}{3H_0^2} A_{GWB}^2 \left( \frac{f}{f_{yr}} \right)^\alpha. \quad (47)$$

The NANOGrav measurements preferred ranges of parameters  $A_{GWB}$  [87] while according to [88]  $\alpha = (5 - \gamma) \in [-1.5, 0.5]$ ,  $f_{yr}$  is best estimated to  $f_{yr} \simeq 3.1 \times 10^{-8}$  and  $H_0$  is given by  $H_0 \equiv 100h \text{ km/s/Mpc}$ .

In Fig. (6), we show the abundance of the energy density of gravitational waves as a function of the present value of the frequency. We also display some expected curves of GW experiments from [89, 90, 91, 92, 93, 94]. We numerically compute the energy spectrum of the induced GWs and test the effect of the preheating duration on the GWs spectrum. The GW spectrum increases the frequencies and spans over some sensitivity curves for  $N_{pre} \leq 2$ .

We conclude that our teleparallel gravity model can explain the energy spectrum at high frequencies for  $N_{pre} \leq 2$  such as ASTROD-GW, BBO and DECIGO. However, higher preheating duration are not consistent with the expected GWs observatories. Unfortunately, our teleparallel gravity model is far away to explain the NANOGrav experiments. Moreover, the parameter  $\delta$  of our  $f(T)$  model can strongly affect the duration of preheating. According to our previous results, the bound  $\delta > 3$  predict higher values of  $N_{pre}$  which can give inconsistent results with the GWs observations curves. Furthermore, the case  $\delta = 3$  provides compatible results with the blue tilted energy spectrum of stochastic gravitational waves for higher frequencies. The reason behind this is that our model of GWs spectrum is derived taking into consideration the phase of preheating rather than inflation alone. Here, we mention that the inflationary gravitational waves are one of the most important stochastic gravitational wave background sources that are used to probe the Universe and can provide possible explanation for the recent NANOGrav results. However, our model predicts higher frequencies because we considered subsequent phases following inflation.

## 7 Conclusion

In this paper, we have reviewed briefly the teleparallel gravity approach in which we have related the slow roll



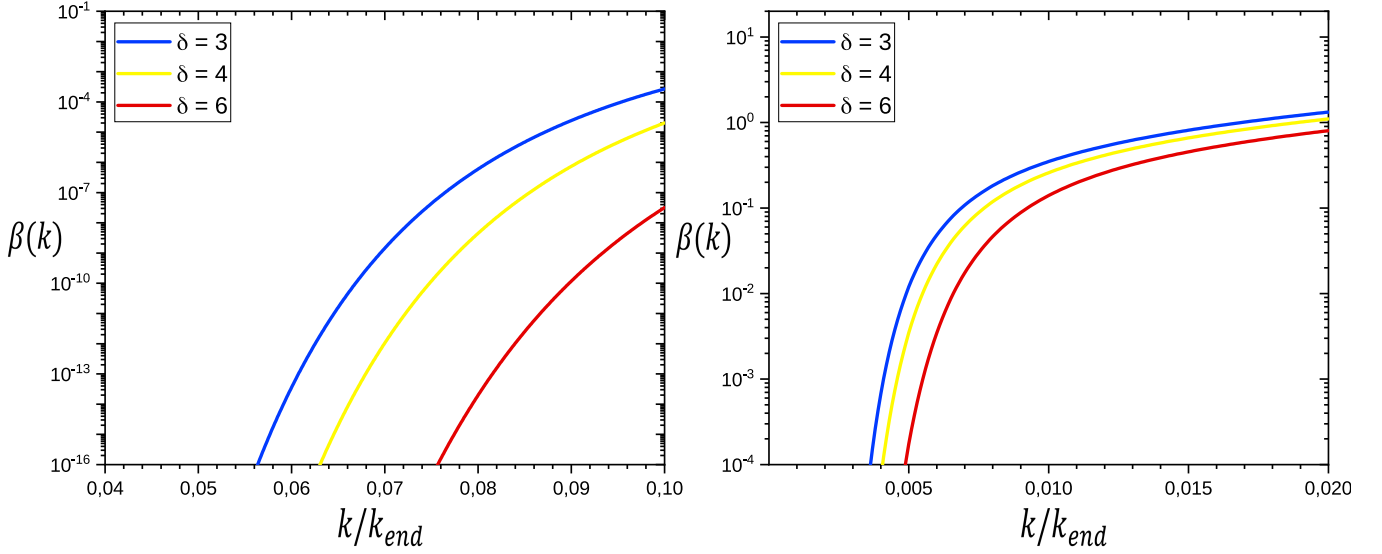


Fig. 5: The fraction of the total energy density collapsing into PBH as functions of dimensionless wavenumber  $k/k_{end}$  for  $\delta = 3$  (blue-line),  $\delta = 4$  (yellow-line) and  $\delta = 6$  (red-line). The left panel presents the case of  $m\Delta t = 50$ , while in the right panel is for  $m\Delta t = 65$ .

and perturbative parameters of the inflationary paradigm. We have also introduced the parametric resonance in the preheating era in which the production of the  $\chi$  fields and the growth of its fluctuations are mandatory for the production of the primordial black holes and gravitational waves.

We have found that, for a chaotic inflation, a good consistency were observed in relation with the  $(r, n_s)$  plane at  $1\sigma$  for and  $2\sigma$  C.L. for some parameters of teleparallel gravity. We have also obtained that the duration of the preheating is consistent with the  $(r, n_s)$  plane at  $1\sigma$  for and  $2\sigma$  C.L..

Moreover, we have also calculated the abundance of primordial black holes produced in the Teleparallel gravity model using the fraction of the energy density and the variance of the density perturbations approach to study PBH collapse. We have found that the primordial black holes overproduction can be satisfied for specific values of the non-adiabatic curvature power spectrum.

We have also obtained that the duration of the preheating is consistent with the observational bound on  $n_s$  and it must be less or equal to 2 explain the present energy density of gravitational waves expected by gravitational waves experiments.

We have calculated the energy spectrum of gravitational waves numerically and have shown that it presents an increasing behavior towards high frequencies. We have shown that for the duration of the preheating equal to 2,

our model may explain the sensitivity curves expected by ASTEOD-GW, BBO and DECIGO. On the other hand, instant transition of preheating i.e.  $N_{pre} = 0$ , our model may explain the sensitivity curves of several gravitational waves experiments, which gives the possibility for our chosen  $f(T)$  model to be examined by the energy spectrum of stochastic gravitational waves observations.

## References

1. C. M. Will, The Confrontation between General Relativity and Experiment, Living Rev. Rel. 17, 4 (2014) [1403.7377].
2. LIGO Scientific, Virgo collaboration, Observation of Gravitational Waves from a Binary Black Hole Merger, Phys. Rev. Lett. 116, 061102 (2016) [1602.03837].
3. LIGO Scientific, Virgo collaboration, Tests of general relativity with GW150914, Phys. Rev. Lett. 116, 221101 (2016) [1602.03841].
4. The LIGO Scientific Collaboration and the Virgo Collaboration collaboration, Tests of general relativity with the binary black hole signals from the ligo-virgo catalog gwtc-1, Phys. Rev. D 100, 104036 (2019).
5. Supernova Cosmology Project collaboration, Measurements of  $\Omega$  and  $\Lambda$  from 42 high redshift supernovae, Astrophys. J. 517, 565 (1999) [astro-ph/9812133].
6. Supernova Search Team collaboration, Observational evidence from supernovae for an accelerating Universe and a cosmological constant, Astron. J. 116, 1009 (1998) [astro-ph/9805201].

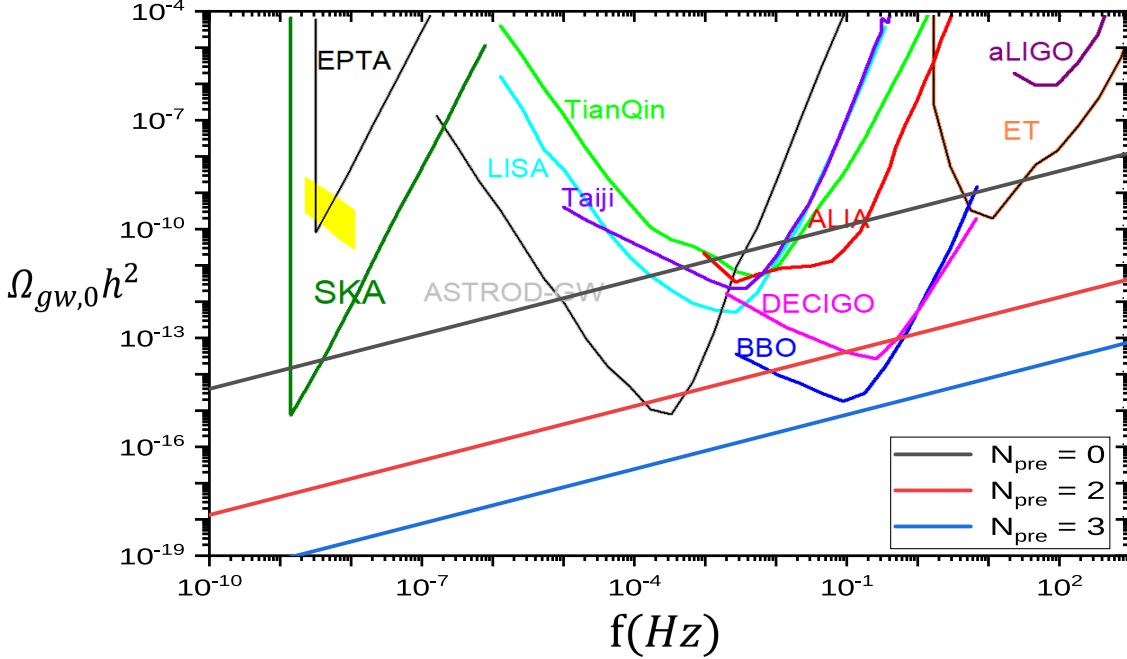


Fig. 6: The abundance of gravity wave energy density as function of the present value of the frequency. We display, from [89,90,91,92,93,94], the sensitivity curves of the Square Kilometer Array (SKA), European Pulsar Timing Array (EPTA), Astrodynamical Space Test of Relativity using Optical-GW detector (ASTROD-GW), Laser Interferometer Space Antenna (LISA), Advanced Laser Interferometer Antenna (ALIA), Big Bang Observer (BBO), Deci-hertz Interferometer GW Observatory (DECIGO), Advanced LIGO (aLIGO) and in yellow NANOGrav 12.5 years experiments. We take  $\alpha = 1/2$  and three different values of preheating duration,  $N_{pre} = 0$  (black), 2 (red) and 3 (blue).

7. WMAP collaboration, First year Wilkinson Microwave Anisotropy Probe (WMAP) observations: Determination of cosmological parameters, *Astrophys. J. Suppl.* 148, 175 (2003) [astro-ph/0302209].
8. D. M. Scolnic et al., The Complete Light-curve Sample of Spectroscopically Confirmed SNe Ia from Pan-STARRS1 and Cosmological Constraints from the Combined Pantheon Sample, *Astrophys. J.* 859, 101 (2018) [1710.00845].
9. Planck collaboration, Planck 2018 results. VI. Cosmological parameters, *Astron. Astrophys.* 641, A6 (2020) [1807.06209].
10. A. H. Guth, The Inflationary Universe: A Possible Solution to the Horizon and Flatness Problems, *Phys. Rev. D* 23, 347-56 (1981).
11. A. D. Linde, The New Inflationary Universe Scenario: A Possible Solution of the Horizon, Flatness, Homogeneity, Isotropy and Primordial Monopole Problems, *Phys. Lett. B* 108, 389-93 (1982).
12. Linde, Andrei. "Inflationary cosmology." *Lect. Notes Phys.* 738, 1-54 (2008) [0705.0164].
13. Gorbunov, Dmitry S., and Valery A. Rubakov. *Introduction to the theory of the early Universe: Cosmological perturbations and inflationary theory.* World Scientific, 2011.
14. Lyth, David H., and Antonio Riotto. "Particle physics models of inflation and the cosmological density perturbation." *Physics Reports*. 314, 1-146 (1999).
15. Aghanim, N., Planck collaboration, Planck 2018 results. VI. Cosmological parameters. 641, A6 (2020) [1807.06209].
16. S. Weinberg, The cosmological constant problem, *Rev. Mod. Phys.* 61 (1989) 1.
17. M. Malquarti, E. J. Copeland and A. R. Liddle, K-essence and the coincidence problem, *Phys. Rev. D* 68, 023512 (2003) [astro-ph/0304277].
18. L. Verde, T. Treu and A. Riess, Tensions between the Early and the Late Universe, *Nature Astron.* 3, 891 (2019) [1907.10625].
19. A. G. Riess, S. Casertano, W. Yuan, J. B. Bowers, L. Macri, J. C. Zinn et al., Cosmic Distances Calibrated to 1% Photometry of 75 Milky Way Cepheids Confirm Tension with  $\Lambda$ CDM, *Astrophys. J. Lett.* 908, L6 (2021) [2012.08534].
20. T. Clifton, P. G. Ferreira, A. Padilla and C. Skordis, Modified Gravity and Cosmology, *Phys. Rept.* 513, 1 (2012) [1106.2476].
21. R. Kase and S. Tsujikawa, Dark energy in Horndeski theories after GW170817: A review, *Int. J. Mod. Phys. D* 28, 1942005 (2019) [1809.08735].
22. T. Kobayashi, Horndeski theory and beyond: a review, *Rept. Prog. Phys.* 82(8), 086901 (2019) [1901.07183].
23. S. Bahamonde, K. F. Dialektopoulos, C. Escamilla-Rivera, G. Farrugia, V. Gakis, M. Hendry et al., Teleparallel Gravity: From Theory to Cosmology, [arXiv:2106.13793v3 [gr-qc]].

24. CANTATA collaboration, Modified Gravity and Cosmology: An Update by the CANTATA Network, [arXiv:2105.12582 [gr-qc]].
25. A. De Felice and S. Tsujikawa, Living Rev. Rel. 13, 3 (2010) [arXiv:1002.4928 [gr-qc]].
26. S. Nojiri and S. D. Odintsov, Phys. Lett. B 631, 1 (2005) [hep-th/0508049].
27. K. Hayashi and T. Nakano, Prog. Theor. Phys. 38, 491–507 (1967).
28. K. Hayashi and T. Shirafuji, Phys. Rev. D 19, 3524 (1979); Addendum-ibid. 24, 3312 (1982).
29. R. Aldrovandi, J.G. Pereira, Teleparallel Gravity: An Introduction, Springer, Dordrecht, 2013.
30. J. W. Maluf, Annalen Phys. 525, 339 (2013) [arXiv:1303.3897 [gr-qc]].
31. Cai, Y. F., Capozziello, S., De Laurentis, M., & Saridakis, E. N., *f(T)* teleparallel gravity and cosmology. Reports on Progress in Physics, 79(10), 106901 (2016).
32. M. Li, R. X. Miao and Y. G. Miao, JHEP 1107, 108 (2011) [arXiv:1105.5934 [hep-th]].
33. K. Bamba, R. Myrzakulov, S. Nojiri and S. D. Odintsov, Phys. Rev. D 85, 104036 (2012) [arXiv:1202.4057 [gr-qc]].
34. Y. P. Wu and C. Q. Geng, Phys. Rev. D 86, 104058 (2012) [arXiv:1110.3099 [gr-qc]].
35. Y. C. Ong, K. Izumi, J. M. Nester and P. Chen, Phys. Rev. D 88, 024019 (2013) [arXiv:1303.0993 [gr-qc]].
36. G. Otalora, JCAP 1307, 044 (2013) [arXiv:1305.0474 [gr-qc]].
37. S. Bahamonde, C. G. Boehmer and M. Wright, Phys. Rev. D 92, no. 10, 104042 (2015) [arXiv:1508.05120 [gr-qc]].
38. K. Rezazadeh, A. Abdolmaleki and K. Karami, JHEP 1601, 131 (2016) [arXiv:1509.08769 [gr-qc]].
39. G. Farrugia and J. L. Said, Phys. Rev. D 94, no. 12, 124054 (2016) [arXiv:1701.00134 [gr-qc]].
40. A. M. Awad, S. Capozziello and G. G. L. Nashed, JHEP 1707, 136 (2017) [arXiv:1706.01773 [gr-qc]].
41. K. Rezazadeh, A. Abdolmaleki and K. Karami, Astrophys. J. 836, 228 (2017) [arXiv:1702.07877 [gr-qc]].
42. Goodarzi, P., & Sadjadi, H. M., Reheating in a modified teleparallel model of inflation. The European Physical Journal C, 79 (3), 1-9 (2019).
43. B. Carr, F. Kuhnel and M. Sandstad, Phys. Rev. D 94, no.8, 083504 (2016) doi:10.1103/PhysRevD.94.083504 [arXiv:1607.06077 [astro-ph.CO]].
44. D. Gaggero, G. Bertone, F. Calore, R. M. T. Connors, M. Lovell, S. Markoff and E. Storm, Phys. Rev. Lett. 118, no.24, 241101 (2017) doi:10.1103/PhysRevLett.118.241101 [arXiv:1612.00457 [astro-ph.HE]].
45. K. Inomata, M. Kawasaki, K. Mukaida, Y. Tada and T. T. Yanagida, Phys. Rev. D 96, no.4, 043504 (2017) doi:10.1103/PhysRevD.96.043504 [arXiv:1701.02544 [astro-ph.CO]].
46. E. D. Kovetz, Phys. Rev. Lett. 119, no.13, 131301 (2017) doi:10.1103/PhysRevLett.119.131301 [arXiv:1705.09182 [astro-ph.CO]].
47. J. Georg and S. Watson, JHEP 09, 138 (2017) doi:10.1007/JHEP09(2017)138 [arXiv:1703.04825 [astro-ph.CO]].
48. Zhou, Z., Jiang, J., Cai, Y. F., Sasaki, M., & Pi, S., Primordial black holes and gravitational waves from resonant amplification during inflation. Physical Review D 102 (10), 103527 (2020).
49. Carr, B., Dimopoulos, K., Owen, C., & Tenkanen, T., Primordial black hole formation during slow reheating after inflation. Physical Review D 97 (12), 123535 (2018).
50. Green, A. M., & Malik, K. A., Primordial black hole production due to preheating. Physical Review D 64 (2), 021301 (2001).
51. K. M. Belotsky, A. D. Dmitriev, E. A. Esipova, V. A. Gani, A. V. Grobov, M. Y. Khlopov, A. A. Kirillov, S. G. Rubin and I. V. Svadkovsky, Mod. Phys. Lett. A 29, no.37, 1440005 (2014) doi:10.1142/S0217732314400057 [arXiv:1410.0203 [astro-ph.CO]].
52. M. Y. Khlopov, Res. Astron. Astrophys. 10, 495-528 (2010) doi:10.1088/1674-4527/10/6/001
53. Lawrence Krauss, Scott Dodelson, and Stephan Meyer. Primordial Gravitational Waves and Cosmology. Science 328, 989-992 (2010).
54. Lev Kofman, Andrei Linde and Alexei A. Starobinsky, "REHEATING AFTER INFLATION", Phys.Rev.Lett.73, 3195-3198 (1994).
55. S. Yu. Khlebnikov and I. I. Tkachev, "Relic gravitational waves produced after preheating", Phys. Rev. D 56 (2), 653 (1997).
56. Jing Liu, Zong-Kuan Guo, Rong-Gen Cai and Gary Shiu, "Gravitational Waves from Oscillons with Cuspy Potentials", Phys. Rev. Lett. 120, 031301 (2018).
57. Richard Easther and Eugene A. Lim, "Stochastic Gravitational Wave Production After Inflation", Journal of Cosmology and Astroparticle Physics 2006(04), 010 (2006).
58. Richard Easther, John T. Giblin, Jr, and Eugene A. Lim, "Gravitational Wave Production At The End Of Inflation", Physical Review Letters 99 (22), 221301 (2007).
59. Pereira, J. G., & Obukhov, Y. N., Gauge structure of teleparallel gravity. Universe 5(6), 139 (2019).
60. Bahamonde, S., Dialektopoulos, K. F., Escamilla-Rivera, C., Farrugia, G., Gakis, V., Hendry, M., ... & Di Valentino, E., Teleparallel gravity: from theory to cosmology. arXiv preprint arXiv:2106.13793 (2021).
61. Basilakos, S., Capozziello, S., De Laurentis, M., Paliathanasis, A., & Tsamparlis, M., Noether symmetries and analytical solutions in *f(T)* cosmology: A complete study. Physical Review D 88 (10), 103526 (2013).
62. Rezazadeh, K., Abdolmaleki, A., & Karami, K., Logamediate inflation in *f(T)* teleparallel gravity. The Astrophysical Journal 836 (2), 228 (2017).
63. Creminelli, P., Nacir, D. L., Simonović, M., Trevisan, G., & Zaldarriaga, M.,  $\phi^2$  or not  $\phi^2$ : testing the simplest inflationary potential. Physical Review Letters 112 (24), 241303 (2014).
64. Green, A. M., & Malik, K. A., Primordial black hole production due to preheating. Physical Review D 64 (2), 021301 (2001).
65. Harada, T., Yoo, C. M., & Kohri, K., Threshold of primordial black hole formation. Physical Review D 88 (8), 084051 (2013).
66. Liddle, A. R., Lyth, D. H., Malik, K. A., & Wands, D., Super-horizon perturbations and preheating. Physical Review D 61 (10), 103509 (2000).
67. El Bourakadi, K., Ferricha-Alami, M., Filali, H., Sakhi, Z., & Bennai, M., Gravitational waves from preheating in Gauss-Bonnet inflation. The European Physical Journal C 81 (12), 1-8 (2021).
68. Kofman, L., Preheating after inflation. In COSMO-97 (pp. 312-321) (1998).

69. Goodarzi, P., & Sadjadi, H. M., Reheating in a modified teleparallel model of inflation. *The European Physical Journal C*, 79(3), 1-9 (2019).
70. Shtanov, Y., Traschen, J., & Brandenberger, R., Universe reheating after inflation. *Physical Review D*, 51(10), 5438 (1995).
71. Mielczarek, J., Reheating temperature from the CMB. *Physical Review D*, 83(2), 023502 (2011).
72. Linde, A., Particle physics and inflationary cosmology (Vol. 5). CRC press (1990).
73. El Bourakadi, K., Bousder, M., Sakhi, Z., & Bennai, M., Preheating and reheating constraints in supersymmetric braneworld inflation. *The European Physical Journal Plus* 136 (8), 1-19 (2021).
74. Carr, B. J., The Primordial black hole mass spectrum, *Astrophysical Journal* 201, 1-19 (1975).
75. Sanchez, N., & Zichichi, A., Current topics in astrophysical physics. *Current topics in astrophysical physics/edited by N. Sanchez*, (1997).
76. Green, A. M., & Liddle, A. R., Constraints on the density perturbation spectrum from primordial black holes. *Physical Review D* 56 (10), 6166 (1997).
77. Bhaumik, N., & Jain, R. K., Primordial black holes dark matter from inflection point models of inflation and the effects of reheating. *Journal of Cosmology and Astroparticle Physics* 2020 (01), 037 (2020).
78. Hertzberg, M. P., & Yamada, M., Primordial black holes from polynomial potentials in single field inflation. *Physical Review D* 97 (8), 083509 (2018).
79. Wu, Y. P., & Geng, C. Q., Matter density perturbations in modified teleparallel theories. *Journal of High Energy Physics* (11), 1-17 (2012).
80. Izumi, K., & Ong, Y. C., Cosmological perturbation in  $f(T)$  gravity revisited. *Journal of Cosmology and Astroparticle Physics* (06), 029 (2013).
81. Cai, Y. F., Li, C., Saridakis, E. N., & Xue, L. Q.,  $f(T)$  gravity after GW170817 and GRB170817A. *Physical Review D* 97 (10), 103513 (2018).
82. J.F. Dufaux, A. Bergman, G. Felder, L. Kofman, J.P. Uzan, Theory and numerics of gravitational waves from preheating after inflation. *Phys. Rev. D* 76.12, 123517 (2007).
83. Lozanov, K. D., & Amin, M. A., Equation of state and duration to radiation domination after inflation. *Physical Review Letters* 119(6), 061301 (2017).
84. Kohri, K., & Terada, T., Solar-mass primordial black holes explain NANOGrav hint of gravitational waves. *Physics Letters B* 813, 136040 (2021).
85. Vaskonen, V., & Veermäe, H., Did NANOGrav see a signal from primordial black hole formation?. *Physical Review Letters* 126 (5), 051303 (2021).
86. De Luca, V., Franciolini, G., & Riotto, A., NANOGrav data hints at primordial black holes as dark matter. *Physical Review Letters* 126 (4), 041303 (2021).
87. Arzoumanian, Z., Baker, P. T., Blumer, H., Bécsy, B., Brazier, A., Brook, P. R., ... & NANOGrav Collaboration., The NANOGrav 12.5 yr data set: search for an isotropic stochastic gravitational-wave background. *The Astrophysical journal letters* 905 (2), L34 (2020).
88. Gao, T. J., & Yang, X. Y., Double peaks of gravitational wave spectrum induced from inflection point inflation. *The European Physical Journal C*, 81 (6), 1-10 (2021).
89. Drees, M., & Xu, Y., Overshooting, critical Higgs inflation and second order gravitational wave signatures. *The European Physical Journal C*, 81 (2), 1-22 (2021).
90. Amaro-Seoane, P., Audley, H., Babak, S., Baker, J., Barausse, E., Bender, P., ... & Zweifel, P., Laser interferometer space antenna., (2017). arXiv preprint arXiv:1702.00786.
91. Ruan, W. H., Guo, Z. K., Cai, R. G., & Zhang, Y. Z., Taiji program: Gravitational-wave sources. *International Journal of Modern Physics A*, 35 (17), 2050075(2020).
92. Moore, C. J., Cole, R. H., & Berry, C. P., Gravitational-wave sensitivity curves. *Classical and Quantum Gravity*, 32 (1), 015014 (2014).
93. Luo, J., Chen, L. S., Duan, H. Z., Gong, Y. G., Hu, S., Ji, J., ... & Zhou, Z. B., TianQin: a space-borne gravitational wave detector. *Classical and Quantum Gravity*, 33 (3), 035010 (2016).
94. Kuroda, K., Ni, W. T., & Pan, W. P., Gravitational waves: Classification, methods of detection, sensitivities and sources. *International Journal of Modern Physics D*, 24 (14), 1530031 (2015).